Neuron
Article

# Calpain-Mediated mGluR1α Truncation: A Key Step in Excitotoxicity

Wei Xu,[1] Tak Pan Wong,[2] Nadege Chery,[2] Tara Gaertner,[2] Yu Tian Wang,[2] and Michel Baudry[1,3,*]
[1] Neuroscience Program, University of Southern California, Los Angeles, CA 90089-2520, USA
[2] Brain Research Center, University of British Columbia, Vancouver, BC V6T 2B5, Canada
[3] Lab address: http://www.usc.edu/programs/neuroscience/faculty/profile.php?fid=21
*Correspondence: baudry@usc.edu
DOI 10.1016/j.neuron.2006.12.020

## SUMMARY

**Excitotoxicity mediated by glutamate receptors plays crucial roles in ischemia and other neurodegenerative diseases. Whereas overactivation of ionotropic glutamate receptors is neurotoxic, the role of metabotropic glutamate receptors (mGluRs), and especially mGluR1, remains equivocal. Here we report that activation of NMDA receptors results in calpain-mediated truncation of the C-terminal domain of mGluR1α at Ser$^{936}$. The truncated mGluR1α maintains its ability to increase cytosolic calcium while it no longer activates the neuroprotective PI$_3$K-Akt signaling pathways. Full-length and truncated forms of mGluR1α play distinct roles in excitotoxic neuronal degeneration in cultured neurons. A fusion peptide derived from the calpain cleavage site of mGluR1α efficiently blocks NMDA-induced truncation of mGluR1α in primary neuronal cultures and exhibits neuroprotection against excitotoxicity both in vitro and in vivo. These findings shed light on the relationship between NMDA and mGluR1α and indicate the existence of a positive feedback regulation in excitotoxicity involving calpain and mGluR1α.**

## INTRODUCTION

Glutamate is the major excitatory neurotransmitter in the brain. Receptors for glutamate consist of three types of ionotropic receptors, namely NMDA, AMPA, and kainate receptors, and three groups of metabotropic receptors. In addition to their physiological roles in normal neurotransmission, glutamate receptors play critical roles in neuronal death resulting from ischemia and other neurodegenerative diseases. Ionotropic glutamate receptors, especially NMDA receptors, have been repeatedly shown to contribute to excitotoxicity. However, the roles of metabotropic glutamate receptors, especially of group I metabotropic glutamate receptors (mGluRI, including mGluR1 and mGluR5), in excitotoxicity remain controversial.

Activation of group I mGluRs appears to be neuroprotective under various conditions. The agonist of group I mGluRs, DHPG, prevented nitric oxide-, hydrogen peroxide-, or platelet-activating factor-induced neurotoxicity in neuronal cultures (Vincent and Maiese, 2000; Zhu et al., 2004). Activation of mGluRs also protected neurons from oxidative stress (Sagara and Schubert, 1998). In organotypic hippocampal slice cultures, mGluR1 activation protected against NMDA-induced excitotoxicity (Blaabjerg et al., 2003). Selective mGluRI blockade exacerbated Aß toxicity (Allen et al., 1999). Recent studies indicated that the neuroprotective effects of mGluRI were mediated by activation of PI$_3$K-Akt signaling through the formation of an mGluRI-Homer-PIKE-L signaling complex (Rong et al., 2003). Activation of Akt and neuroprotection by mGluRI were also reported in other studies (Hou and Klann, 2004; Chong et al., 2006).

Numerous experiments demonstrate neurotoxic effects of mGluRI activation, however. In models of cerebral ischemia, activation of mGluRI, especially of mGluR1, is neurotoxic, while antagonists of mGluR1 are neuroprotective. The neurotoxic effects of mGluR1 activity in ischemia might be due to their effects on cytosolic free $Ca^{2+}$ and their stimulation of glutamate release (Pellegrini-Giampietro, 2003).

Because multiple types of glutamate receptors are simultaneously activated under excitotoxic conditions, interactions between receptors might play important roles in determining the outcome of toxic insults. The present study was therefore directed at evaluating interactions between NMDA and mGluR1α receptors. Our results indicate that overactivation of NMDA receptors alters signaling mechanisms and roles in excitotoxicity of mGluR1α through calpain-mediated truncation.

## RESULTS

### NMDA Receptor Activation Induces C-Terminal Truncation of mGluR1α

To detect possible mGluR1α modifications following glutamate-induced excitotoxicity, cultured cortical neurons (14–18 days in vitro; DIV) were incubated with glutamate (100 μM) for 1–60 min. Total cell lysate was collected

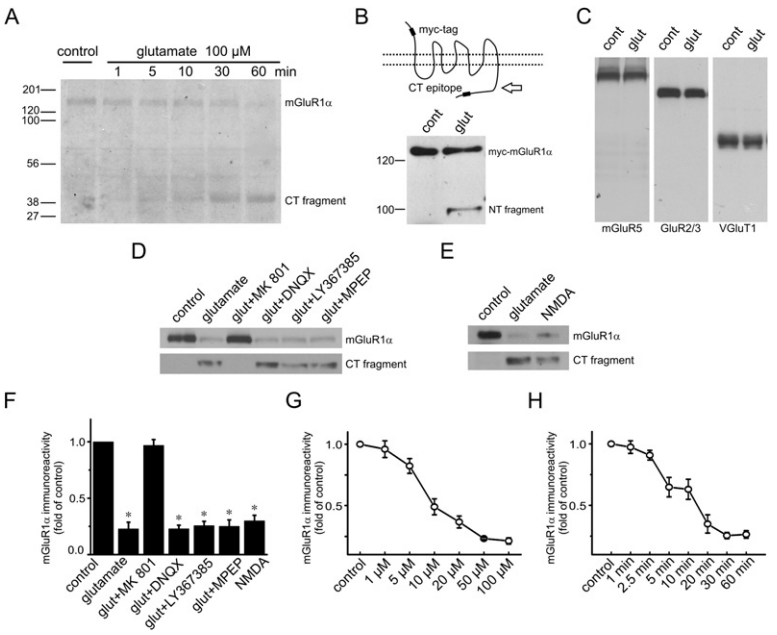


**Figure 1. Glutamate Induces C-Terminal Truncation of mGluR1α as a Result of NMDA Receptor Activation**

(A) Neurons were treated with glutamate for the indicated periods of time. Total cell lysates were blotted with an antibody against the C terminus of mGluR1α (mGluR1$\alpha_{1142–1160}$).

(B) Neurons were transfected with myc-mGluR1α and treated with glutamate. Total cell lysates were probed with anti-myc antibody (the schematic shows locations of epitopes; the arrow indicates the putative cleavage site).

(C) Neurons were treated with glutamate and whole lysates were blotted with antibodies against mGluR5, GluR2/3, and VGluT1.

(D and F) Representative blot and quantification of the effects of an NMDA receptor antagonist on glutamate-induced truncation of mGluR1α. Neurons were treated with glutamate alone (n = 7) or glutamate + MK 801 (n = 4), DNQX (n = 5), LY367385 (n = 4), or MPEP (n = 4). Total cell lysates were blotted with anti-mGluR1$\alpha_{1142–1160}$.

(E and F) NMDA induced a similar truncation of mGluR1α. Neurons were treated with glutamate or NMDA (n = 5) and whole lysates were blotted with anti-mGluR1$\alpha_{1142–1160}$. Results are means ± SEM. *$p < 0.001$, Student's t test.

(G and H) Concentration and time dependency of NMDA-induced truncation of mGluR1α. Cortical neurons were treated for 1 hr with the indicated concentrations of NMDA (G) or were treated with 10 μM NMDA for the indicated periods of time (H). Results are means ± SEM of four experiments.

immediately after treatment and subjected to SDS-PAGE and immunoblotting with an antibody against the carboxyl terminus (residues 1142–1160) of mGluR1α (Figure 1A). Levels of full-length mGluR1α decreased with increasing incubation time, while levels of a low-molecular weight band at about 38 kDa increased, suggesting that truncation of mGluR1α occurred at the C terminus. To probe the amino terminus of mGluR1α after truncation, cortical neurons were transfected with an mGluR1α construct tagged with a myc epitope at the N terminus (myc-mGluR1α, the EQKLISEEDL epitope, was inserted in-frame after $Ala^{30}$ of mGluR1α; Francesconi and Duvoisin, 2002) after 3 days in vitro. Neurons were transfected with a calcium phosphate precipitation method modified for high transfection rate (Jiang et al., 2004). One week later, transfected neurons were treated with 100 μM glutamate for 1 hr and total lysates were processed for western blots. When probed with an anti-myc antibody, blots revealed a low-molecular weight band at about 100 kDa after glutamate treatment (Figure 1B), which corresponds to the N-terminal fragment after truncation. The optical density of the original myc-mGluR1α did not decrease significantly, suggesting that only a small fraction of overexpressed myc-mGluR1α was cleaved. Because the apparent molecular weight of mGluR1α on SDS-PAGE is about 140 kDa, our data suggested that glutamate induced truncation of mGluR1α in the C terminus, most likely at a single cleavage site.

To test for the specificity of glutamate-mediated truncation of mGluR1α, immunoblots were also probed with an antibody against mGluR5, another member of group I mGluRs, which shares a high similarity with mGluR1α. As shown in Figure 1C, levels of mGluR5 were not significantly altered by glutamate. Similarly, no significant changes occurred to the GluR2/3 subunits of AMPA receptors, or to the vesicular glutamate transporter (VGluT1), a presynaptic protein in glutamatergic synapses.

Selective glutamate receptor antagonists were used to identify the glutamate receptor(s) involved in mGluR1α truncation. Glutamate (100 μM, 1 hr) induced a significant reduction in the levels of mGluR1α. An NMDA receptor antagonist, MK-801 (10 μM), completely blocked this effect, whereas the non-NMDA glutamate receptor antagonist, DNQX (100 μM), had no effect. Similarly, mGluR1 blockade with LY367385 (100 μM) or mGluR5 blockade with MPEP (100 μM) did not prevent truncation (Figures 1D and 1F). Furthermore, when cortical neurons were treated with NMDA (50 μM, 1 hr), a similar degree of mGluR1α truncation was produced (Figure 1E). To characterize NMDA-induced mGluR1α truncation, concentration and time dependencies of NMDA effects were studied. Cortical neurons were first incubated with 1–100 μM NMDA for a fixed period of time (1 hr) (Figure 2G). The minimum concentration of NMDA required to induce significant mGluR1α truncation was 10 μM ($p < 0.001$, n = 4, Student's t test for control versus 10 μM). In a following experiment, cortical neurons were incubated with 10 μM NMDA for 1–60 min (Figure 2H). The minimum time required for 10 μM NMDA to induce truncation was 5 min ($p < 0.01$, n = 4, Student's t test for control versus 5 min). In summary, these data indicate that activation of NMDA receptors but not non-NMDA glutamate receptors results in

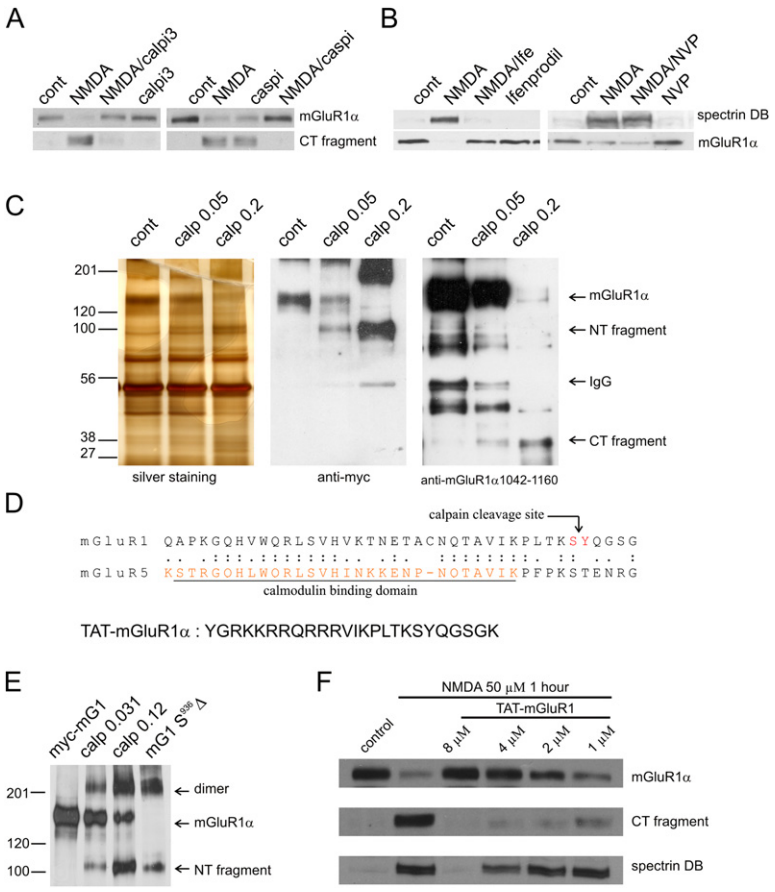


**Figure 2. mGluR1α Is Truncated by Calpain at Ser$^{936}$**

(A) NMDA-induced truncation of mGluR1α was significantly blocked by calpain inhibitor III (Calpi3) but not by caspase inhibitor cpm-VAD-CHO (Caspi).

(B) Calpain was activated by NMDA. Neurons were treated as indicated and total cell lysates were blotted with anti-spectrin or anti-mGluR1α$_{1142–1160}$, respectively. Only the degradation bands of spectrin (spectrin DB, at ~145 kD) are shown. NMDA-induced spectrin degradation and mGluR1α truncation were blocked by ifenprodil but not by NVP-AAM077.

(C) Immunoprecipitated myc-mGluR1α was digested with μ-calpain at the indicated concentrations (U/ml) for 30 min. The digested material was processed for SDS-PAGE and subjected to silver staining or immunoblots. With silver staining, myc-mGluR1α (~140 kDa) was cleaved by calpain into two bands of molecular weight 100 kDa (corresponding to the N-terminal fragment, as it was detected with the anti-myc antibody) and 38 kDa (corresponding to the C-terminal fragment, as it was detected with anti-mGluR1α$_{1142–1160}$).

(D) Alignment of mGluR1 (residues 902–941) and mGluR5 (residues 889–927) sequences surrounding the calpain cleavage site and sequence of the TAT-mGluR1 peptide. The calpain cleavage site was identified by sequencing calpain-digested GST-mGluR1$_{889–1058}$ fusion protein. The TAT-mGluR1 peptide was designed to generate a cell-permeable (by TAT PTD sequence) peptide that contains a sequence that overlaps the calpain cutting site in mGluR1α.

(E) Immunoblot probed with anti-myc antibody showing that myc-mGluR1αS$^{936}$Δ exhibited the same molecular weight as the N-terminal fragment of calpain-cleaved myc-mGluR1α. Lane 1 shows myc-mGluR1α immunoprecipitated from HEK293 cells, lanes 2 and 3 show myc-mGluR1α digested with increasing calpain concentrations, and lane 4 shows myc-mGluR1αS$^{936}$Δ.

(F) TAT-mGluR1 peptide blocked NMDA-induced mGluR1α truncation. Neurons were pretreated with the TAT-mGluR1 peptide or vehicle followed by NMDA, and total cell lysates were blotted with anti-mGluR1α$_{1142–1160}$ or anti-spectrin antibodies.

mGluR1α truncation and that mGluR1α truncation requires prolonged activation of NMDA receptors.

## mGluR1α Is Truncated by Calpain at Ser$^{936}$

We then determined which protease(s) mediated NMDA-induced mGluR1α truncation. Previous studies have indicated that both the calcium-dependent neutral protease calpain and caspases could be activated by neurotoxic concentrations of NMDA. Cortical neurons were pretreated with a calpain inhibitor, the cell-permeable calpain inhibitor III (10 μM), or the caspase inhibitor cpm-VAD-CHO for 2 hr followed by 50 μM NMDA for 1 hr. Pretreatment with calpain inhibitor III significantly blocked NMDA-induced truncation (Figure 2A), while cpm-VAD-CHO had no effect. To confirm the activation of calpain by NMDA under our experimental conditions, we determined the levels of spectrin degradation fragments. The 145 kDa spectrin degradation band (spectrin DB), which is widely used as a marker of calpain activation, could not be detected under control conditions but appeared after treatment with NMDA (Figure 2B). In addition, NMDA-induced spectrin degradation could be blocked by ifenprodil (10 μM), a selective antagonist of NR2B subunit-containing NMDA receptors, but not by NVP-AAM077 (0.4 μM), a selective antagonist for NR2A subunit-containing NMDA receptors. Similarly, NMDA-induced mGluR1α truncation was selectively blocked by ifenprodil but not by NVP-AAM077. Note that under these conditions, the 120 kDa spectrin degradation fragment generated by caspase-induced spectrin truncation (Newcomb et al., 2000) was never observed, further strengthening the conclusion that calpain but not caspase was responsible for mGluR1α truncation.

The involvement of calpain in mGluR1α truncation did not necessarily imply that calpain could directly cleave the C terminus of mGluR1α. To confirm that mGluR1α truncation is directly mediated by calpain, we first transfected HEK293 cells with the N-terminal myc-epitope-tagged mGluR1α. Two days later, mGluR1α was immunoprecipitated with anti-mGluR1α C-terminal antibody and incubated with different concentrations of μ-calpain for

30 min. Aliquots of precipitated proteins were processed for SDS-PAGE and silver staining, and the rest of the samples were used for western blots with antibodies against the myc epitope or mGluR1α C terminus, respectively (Figure 2C). With silver staining, the density of the 145 kDa band that represents full-length mGluR1α decreased dose dependently with calpain treatment. In parallel, two additional bands appeared after calpain treatment, with apparent molecular weights of 100 kDa and 38 kDa, respectively. The 100 kDa band proved to be the N terminus of mGluR1α derived from truncation, as it reacted with the anti-myc antibody. Likewise, the 38 kDa protein proved to be the C terminus of mGluR1α, as it was labeled with the anti-mGluR1α C-terminal antibody. These data indicated that calpain could directly cleave mGluR1α at the C terminus.

From the size of mGluR1α fragments after cleavage, we deducted that the calpain cleavage site in mGluR1α should be between residue $I^{812}$ (the molecular weight of the sequence from $I^{812}$ to the C terminus is 38.25 kDa) and $S^{943}$ (the molecular weight from the N terminus to $Ser^{943}$ is 105.62 kDa). We therefore made a GST fusion protein containing the sequence of mGluR1α from $I^{812}$ to $S^{943}$. The GST fusion protein was expressed in and purified from BL21 *Escherichia coli* and digested with calpain. This fusion protein became about 2 kDa smaller after digestion, suggesting that the cleavage site was close to $S^{943}$. To get enough C-terminal fragment for Edman protein sequencing, another construct was made by fusing the mGluR1α sequence from $N^{889}$ to $L^{1058}$ to the C terminus of GST. As expected, after digestion with calpain, this fusion protein generated a 10 kDa fragment. The N terminus of this fragment was sequenced to be YQGS with Edman degradation, indicating that the calpain cleavage site in mGluR1α is between $S^{936}$ and $Y^{937}$ (Figure 2D). The molecular weight (MW) of mGluR1α from residues 1–936 is 104.87 kDa, which matches well with the apparent MW of the N-terminal fragment after truncation. The MW of mGluR1α residues 937–1199 is 28.41 kDa, which is lower than the 38 kDa apparent MW of the C-terminal fragment. However, the C-terminal domain of mGluR1α has a high percentage of proline (45 out of the 263 amino acids), with some proline-rich domains composed solely of prolines. Proline-rich proteins normally show higher apparent MW on SDS-PAGE, which might explain the seemingly different molecular weights of the C-terminal fragment. To obtain further confirmation of this truncation site, a stop codon was introduced into the myc-mGluR1α plasmid immediately after $Ser^{936}$ to generate a construct for truncated mGluR1α (myc-mGluR1α$S^{936}$Δ). Transfected in HEK293 cells, this construct generated a protein with the same apparent molecular weight (~100 kDa) as the mGluR1α N-terminal fragment generated after calpain-mediated truncation (Figure 2E).

To selectively block calpain-mediated truncation of mGluR1α, a peptide was constructed by fusing the mGluR1α sequence spanning the calpain cleavage site with the TAT protein transduction domain, a procedure that has been used to transfer material across cell membranes (Wadia et al., 2004). We reasoned that this peptide would compete with endogenous mGluR1α for calpain and therefore protect it from truncation. Incubation of brain membrane fractions with calpain resulted in truncation of both mGluR1α and spectrin. The TAT-mGluR1 fusion peptide dose dependently reduced calpain-mediated truncation of mGluR1α but not of spectrin. The TAT peptide itself showed no significant effect on calpain-mediated truncation of mGluR1α or spectrin (see Supplemental Data available with this article online). We then tested the effect of the peptide on cultured neurons. Cortical cultures were incubated with different concentrations of TAT-mGluR1 for 90 min followed by 50 μM NMDA for 1 hr. As shown in Figure 2F, treatment with the peptide resulted in a dose-dependent inhibition of NMDA-induced mGluR1α truncation. At the lower concentrations (1–2 μM), the peptide significantly reduced mGluR1α truncation with little effect on spectrin degradation, while at higher concentrations (4–8 μM), spectrin degradation was also blocked.

## C-Terminal Truncated mGluR1α Remains Functional

The main signaling mechanism activated by mGluR1α consists of PI hydrolysis through G protein and phospholipase C, which eventually leads to calcium release from internal calcium stores. Therefore, we first performed calcium imaging to determine whether mGluR1α remains functional following C-terminal truncation. Wild-type mGluR1 (myc-mGluR1α) or the truncated form (myc-mGluR1α$S^{936}$Δ) was cotransfected with DsRED (red fluorescent protein) into HEK293 cells. Two days after transfection, cells were loaded with a calcium reporter, Oregon green 488 BAPTA-1 AM (0.63% in extracellular solution). As shown in Figure 3, a significant increase in intracellular calcium concentration could be detected after treatment of cells transfected with myc-mGluR1α with 100 μM DHPG, a selective agonist for group I mGluRs (maximum $\Delta F/F = 30.6 \pm 4.2\%$; $n = 8$). This calcium response requires mGluR1α activation because no change in fluorescent signals could be observed in nontransfected cells. In cells transfected with myc-mGluR1α$S^{936}$Δ, DHPG could induce qualitatively similar, although significantly smaller, calcium transients (maximum $\Delta F/F = 20.1 \pm 2.1\%$; $n = 10$; $p < 0.05$, Student's t test for myc-mGluR1α versus myc-mGluR1α$S^{936}$Δ). These data indicated that mGluR1α remains functional following C-terminal truncation at $Ser^{936}$.

## C-Terminal Truncation Alters mGluR1α Signaling

Activation of mGluR1α can also stimulate nonselective cation excitatory postsynaptic conductance. We therefore analyzed mGluR1α-dependent currents before and after calpain-mediated truncation. We transfected HEK293 cells with either myc-mGluR1α or myc-mGluR1α$S^{936}$Δ plus GIRK1, GIRK2 or TRPC1. Application of DHPG evoked an inward current in HEK293 cells transfected with myc-mGluR1α and either TRPC1 or GIRK1, 2. Mean

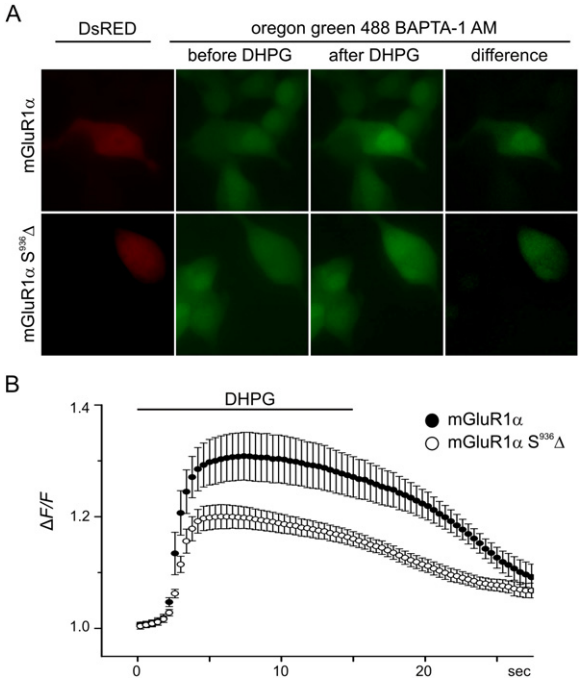


**Figure 3. C-Terminal Truncated mGluR1α Remains Functional for Increasing Cytosolic Free Calcium**

HEK293 cells were cotransfected with DsRED and myc-mGluR1α or myc-mGluR1αS$^{936}$Δ. DHPG was used to induce mGluR1α-mediated calcium transient.

(A) Photos on the left show expression of DsRED, which labels transfected cells; photos in the middle illustrate the fluorescent signal obtained with the calcium indicator Oregon green 488 BAPTA-1 AM before and after DHPG application; photos on the right are obtained by subtracting "before DHPG" from "after DHPG," thus representing DHPG-induced calcium transients.

(B) Quantification of DHPG-induced calcium transients in myc-mGluR1α- or myc-mGluR1αS$^{936}$Δ-transfected cells; results are means ± SEM of eight to ten experiments.

amplitude of DHPG-induced current in myc-mGluR1α/TRPC1-transfected cells was −36.7 ± 9.6 pA (mean ± SEM, n = 7 cells), while in myc-mGluR1α/GIRK1, 2-transfected cells, average amplitude of whole-cell current was −24.2 ± 6.3 pA (n = 5 cells). In contrast, whole-cell currents were markedly reduced or absent in cells transfected with myc-mGluR1αS$^{936}$Δ, with a mean amplitude of −9.7 ± 6.8 pA in myc-mGluR1αS$^{936}$Δ/TRPC1-transfected cells (n = 5) and −1.4 ± 0.8 pA in myc-mGluR1-αS$^{936}$Δ/GIRK1, 2-transfected cells (n = 3). As illustrated in Figure 4A, whole-cell response induced by wild-type mGluR1α was significantly greater than that mediated by truncated mGluR1α ($p < 0.05$, Student's t test for myc-mGluR1α versus myc-mGluR1αS$^{936}$Δ in both TRPC1- and GIRK1, 2-transfected cells).

As reported in previous studies, mGluR1 activation can stimulate the $PI_3K$-Akt signaling pathway through the mGluRI-Homer-PIKE-$PI_3K$ signaling complex. Therefore, we tested whether this signaling mechanism remained functional after mGluR1α truncation. We first induced mGluR1α truncation by treating cortical neurons with 50 μM NMDA for 1 hr. Two hours after washing out NMDA, neurons were incubated with DHPG (50 μM) for 10 min. Neurons were then lysed and levels of Akt phosphorylation were determined with western blots by calculating the ratio of phosphorylated Akt to total Akt. DHPG induced a moderate increase in Akt phosphorylation levels in neurons ($p < 0.05$, n = 6, Student's t test for cont1 versus DHPG1) (Figure 4B). Pretreatment with NMDA reduced basal levels of phosphorylated Akt ($p < 0.001$, n = 6, Student's t test for cont1 versus cont2). Under this condition, DHPG failed to increase Akt phosphorylation levels ($p = 0.27$, n = 6, Student's t test for cont2 versus DHPG2). When neurons were pretreated with 8 μM TAT-mGluR1 for 90 min to block mGluR1α truncation, NMDA-induced reduction of Akt phosphorylation was partially reversed ($p < 0.05$, n = 6, Student's t test for cont3 versus cont2). More importantly, DHPG-induced increase of Akt phosphorylation was restored ($p < 0.05$, n = 6, Student's t test for cont3 versus DHPG3). Together, the data indicated that the mGluR1α-$PI_3K$-Akt signaling pathway was disrupted by calpain-mediated mGluR1α truncation and that preventing truncation with the TAT-mGluR1 peptide restored this signaling mechanism.

## C-Terminal Truncation Alters mGluR1α Targeting in Cortical Neurons

Previous studies have shown that the C-terminal domain of mGluR1α is crucial for its dendritic localization. Therefore, it was interesting to determine whether mGluR1α targeting was modified following calpain-mediated truncation. Cortical neurons were transfected with myc-mGluR1α. After 48 hr, neurons were treated with 50 μM NMDA or vehicle for 1 hr. After 3 hr of washing out NMDA, neurons were fixed and stained with antibodies against the N-terminal myc epitope or the C terminus of mGluR1α, respectively. Full-length mGluR1α was selectively targeted to dendrites and almost excluded from axons (Figure 5A). But in ~34% of neurons treated with NMDA (124 out of 367 neurons counted), myc immunoreactivity could be detected in axons, especially in the proximal segment, whereas immunoreactivity for the C terminus of mGluR1α was still restricted to dendrites (Figure 5B). These results indicated that NMDA-induced C-terminal truncation altered mGluR1α targeting.

To test whether NMDA-induced translocation of mGluR1α from dendrites to axons was an active process or passive diffusion after truncation, we transfected cortical neurons with myc-mGluR1αS$^{936}$Δ. Targeting of mGluR1-αS$^{936}$Δ 48 hr after transfection was dramatically different from that of full-length mGluR1α (Figure 5C). In the majority of transfected neurons (~73%, 500 out of 681 neurons counted), immunoreactivity for myc tag was strictly restricted to cell bodies (Figure 5C, upper panel). The cell-body restriction was the same when immunostaining was performed 6 days after transfection, suggesting that it was not the result of a delay in expression or delivery but rather mediated by targeting signals. In a smaller fraction

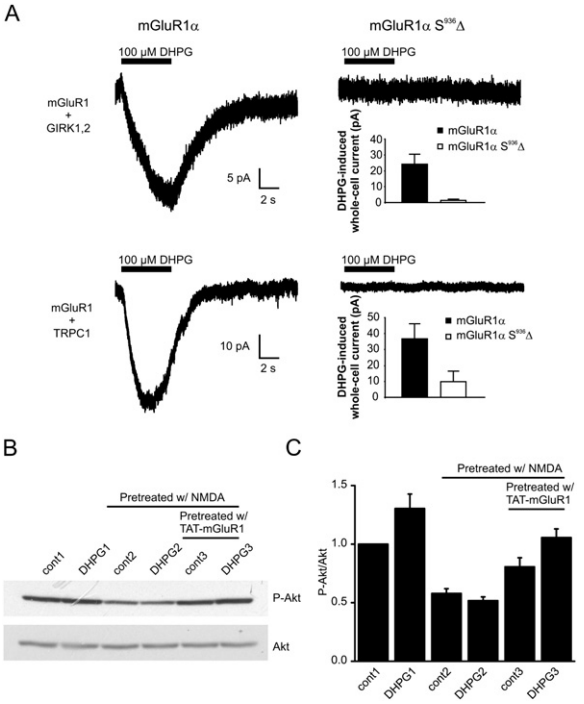


**Figure 4. C-Terminal Truncation Alters mGluR1α Signaling**

(A) Recordings of mGluR1-induced whole-cell currents in HEK293 cells. Representative current traces recorded from HEK293 cells transfected with either myc-mGluR1α (left panel) or myc-mGluR1αS$^{936}$Δ (right panel) and GIRK1, GIRK2 (top) or TRPC1 (bottom). DHPG (100 μM in extracellular solution) was applied using a fast perfusion system for the period indicated by the scale bars. Each trace is the average of five continuous sweeps. Bar graphs represent means ± SEM of DHPG-induced current amplitude recorded in cells transfected with myc-mGluR1α or myc-mGluR1αS$^{936}$Δ + GIRK1, GIRK2 (top right) or TRPC1 (bottom right) (n = 3–7).

(B and C) Representative blots (B) and quantification (C) showing alterations of mGluR1-Akt signaling by calpain-mediated truncation.

DHPG induced a moderate increase in Akt phosphorylation levels in neurons ($p < 0.05$, cont1 versus DHPG1, n = 6). Pretreatment with NMDA reduced levels of phosphorylated Akt ($p < 0.001$, cont1 versus cont2, n = 6) and abolished DHPG effect ($p = 0.27$, cont2 versus DHPG2, n = 6). Pretreatment with TAT-mGluR1 partially blocked NMDA-induced reduction in levels of phosphorylated Akt ($p < 0.05$, cont3 versus cont2, n = 6) and restored the effect of DHPG in activating Akt ($p < 0.05$, cont3 versus DHPG3, n = 6).

of neurons (~22%, 150 out of 681 neurons counted), mGluR1α was selectively targeted to axons (Figure 5C, middle panel). There were also a few neurons (~4.5%, 31 out of 681 neurons counted) where immunostaining appeared in dendrites. However, in contrast to the even distribution of full-length mGluR1α in dendrites, truncated mGluR1α formed large clusters (Figure 5C, bottom panel).

## Distinct and Opposite Roles of Wild-Type and Truncated mGluR1α in Excitotoxicity

Calpain-mediated mGluR1α truncation was induced mainly by toxic concentrations of NMDA. The downstream signaling pathways of mGluR1α, including intracellular calcium release and activation of $PI_3K$-Akt, are both important for excitotoxicity. Therefore, we postulated that NMDA-induced truncation would alter the role of mGluR1α in neuronal toxicity. To test this possibility, we first cotransfected neurons with green fluorescent protein (GFP) and a control vector, wild-type mGluR1α, or truncated mGluR1α. Two days later, neurons were treated with 25 μM glutamate for 1 hr. Twelve hours after treatment, neurons were stained with 0.5 μM ethidium homodimer 1 (EthD-1) for 10 min to label nuclei of dead cells. Numbers of GFP-expressing neurons and EthD-1-positive GFP-expressing neurons on each 18 × 18 mm coverslip were counted to calculate the percentage of dead cells. Toxic effects of glutamate treatment could readily be observed in most GFP-expressing neurons, which exhibited significant neurite retraction (Figures 6A and 6B). In neurons cotransfected with control vector, 35% (n = 9; an average of 405 GFP-expressing neurons were counted on each coverslip) of GFP-expressing neurons were positive for EthD-1 staining and therefore had died. In neurons cotransfected with wild-type mGluR1α, only 15% of neurons (n = 8; an average of 428 GFP-expressing neurons were counted on each coverslip) were EthD-1 positive, an effect that was statistically different from that in neurons cotransfected with control vector ($p < 0.01$, Student's t test). In contrast, 59% of neurons cotransfected with mGluR1αS$^{936}$Δ (n = 9; an average of 439 GFP-expressing neurons were counted on each coverslip) were EthD-1 positive, an effect significantly higher than observed in neurons cotransfected with control vector ($p < 0.05$, Student's t test). The opposite effects of wild-type and truncated mGluR1α indicated that wild-type and truncated mGluR1α have distinct roles in excitotoxicity.

We then tested whether calpain-mediated truncation of endogenous mGluR1α also alters its role in excitotoxicity. We used NMDA to elicit mGluR1α truncation and evaluated the role of mGluR1 in neuronal toxicity by applying DHPG before and after truncation. Cortical neurons cultured on 18 × 18 mm coverslips were divided into six groups which received the following treatments: (1) *control*, vehicle; (2) *NMDA*, 100 μM NMDA for 1 hr; (3) *DHPG before NMDA*, DHPG, 100 μM for 1 hr, followed by 100 μM NMDA for 1 hr; (4) *DHPG after NMDA*, NMDA, 100 μM for 1 hr, followed by 100 μM DHPG for 1 hr; (5) *DHPG + LY before NMDA*, 100 μM DHPG was coapplied with 100 μM LY367385 for 1 hr followed by 100 μM NMDA for 1 hr; (6) *DHPG + LY after NMDA*, NMDA, 100 μM for 1 hr, followed by 100 μM DHPG coapplied with 100 μM LY367385. One day after treatment, all neurons were stained for 20 min with 0.5 μM EthD-1 to label dead cells and 2 μM calcein AM to label live cells. After washes, coverslips were mounted and one microscopy photo was immediately taken of the center area of each coverslip. EthD-1- and calcein AM-positive cells in each photo were then counted. The percentage of dead cells was calculated as the number of EthD-1-positive cells/(number of EthD-1-positive cells + number of calcein

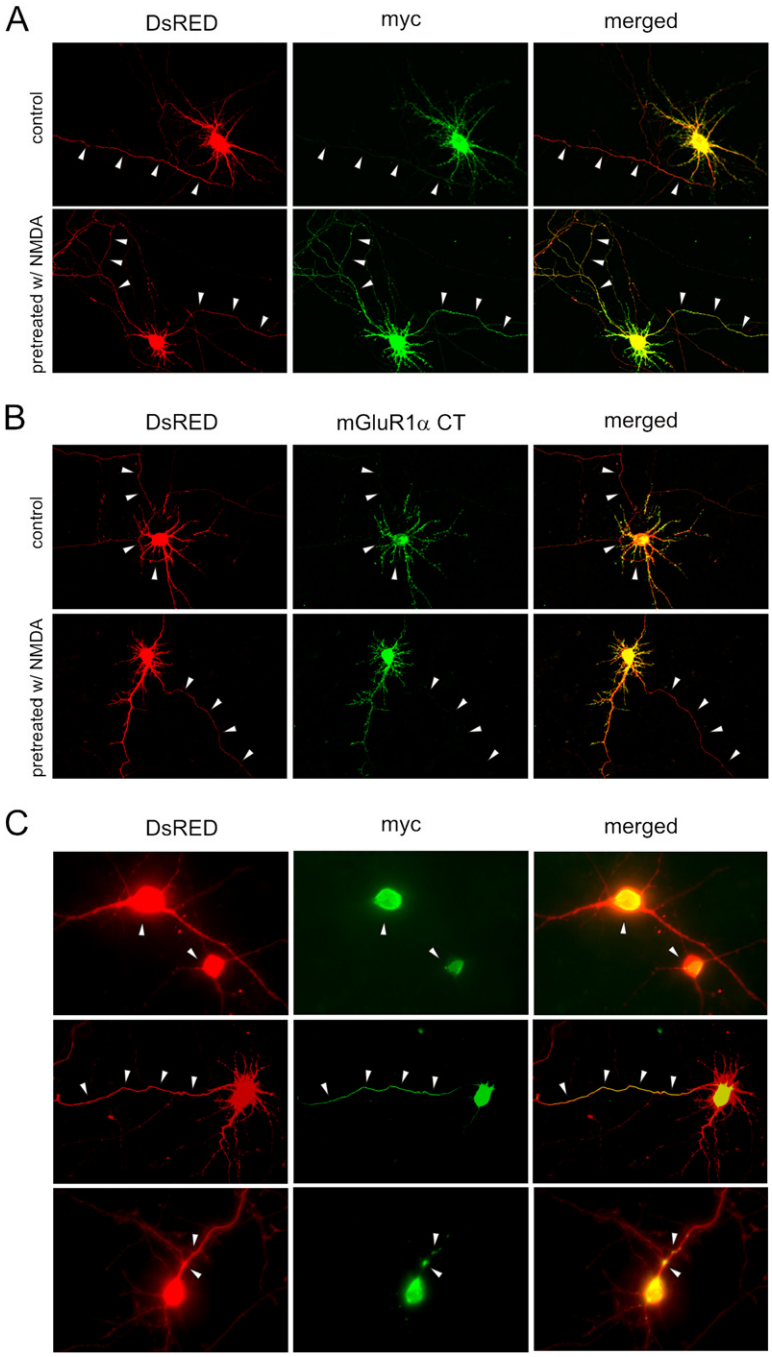


**Figure 5. C-Terminal Truncation Alters mGluR1α Targeting**

(A and B) Neurons were cotransfected with DsRED and myc-mGluR1α. After 48 hr, neurons were fixed and stained with anti-myc (A) or anti-mGluR1$\alpha_{1142–1160}$ (B) and anti-DsRED antibodies. Myc-mGluR1α (upper panel) was not present in axons (arrowheads) under control conditions. After treatment with NMDA (lower panel), myc-tag staining appeared in the proximal segment of axons (A), while staining of the mGluR1α C terminus was still absent in axons (B).

(C) Neurons were cotransfected with DsRED and myc-mGluR1α$S^{936}\Delta$. Neurons were stained with anti-myc and anti-DsRED antibodies 48 hr later. In ~73% of neurons, myc immunoreactivity was restricted to cell bodies (upper panel; arrowheads point to cell bodies); in ~20% of neurons, myc-mGluR1α$S^{936}\Delta$ was preferentially targeted to axons (middle panel; arrowheads point to axons). In ~5% of neurons, myc-mGluR1α$S^{936}\Delta$ was preferentially targeted to dendrites and formed large clusters (lower panel; arrowheads point to clusters in dendrites).

AM-positive cells) *100%. As shown in Figures 6C and 6D, *control* had 8% cell death (n = 12). In *NMDA*, cell-death rate increased to 37% (n = 12), which was significantly higher than that in *control* ($p < 0.001$, Student's t test), indicating toxicity of NMDA; 29% cell death was found in *DHPG before NMDA* (n = 9), which was significantly lower than that of *NMDA* ($p < 0.001$, Student's t test), suggesting a neuroprotective effect of DHPG under this condition. This effect was blocked by coapplying LY367385 (*DHPG + LY before NMDA*, 35.1% cell death, n = 11; $p < 0.05$ compared with *DHPG before NMDA*; $p = 0.38$ compared with *NMDA*, Student's t test), indicating that it was mediated by mGluR1. *DHPG after NMDA* had 54% cell death (n = 12), which was significantly higher than that of *NMDA* ($p < 0.001$, Student's t test), indicating a neurotoxic effect of DHPG treatment under this condition. This toxic effect was blocked by coapplying LY367385 (*DHPG + LY after NMDA*, 39.9% cell death, n = 9; $p < 0.001$ compared with *DHPG after NMDA*; $p = 0.27$ compared with *NMDA*, Student's t test). The opposite

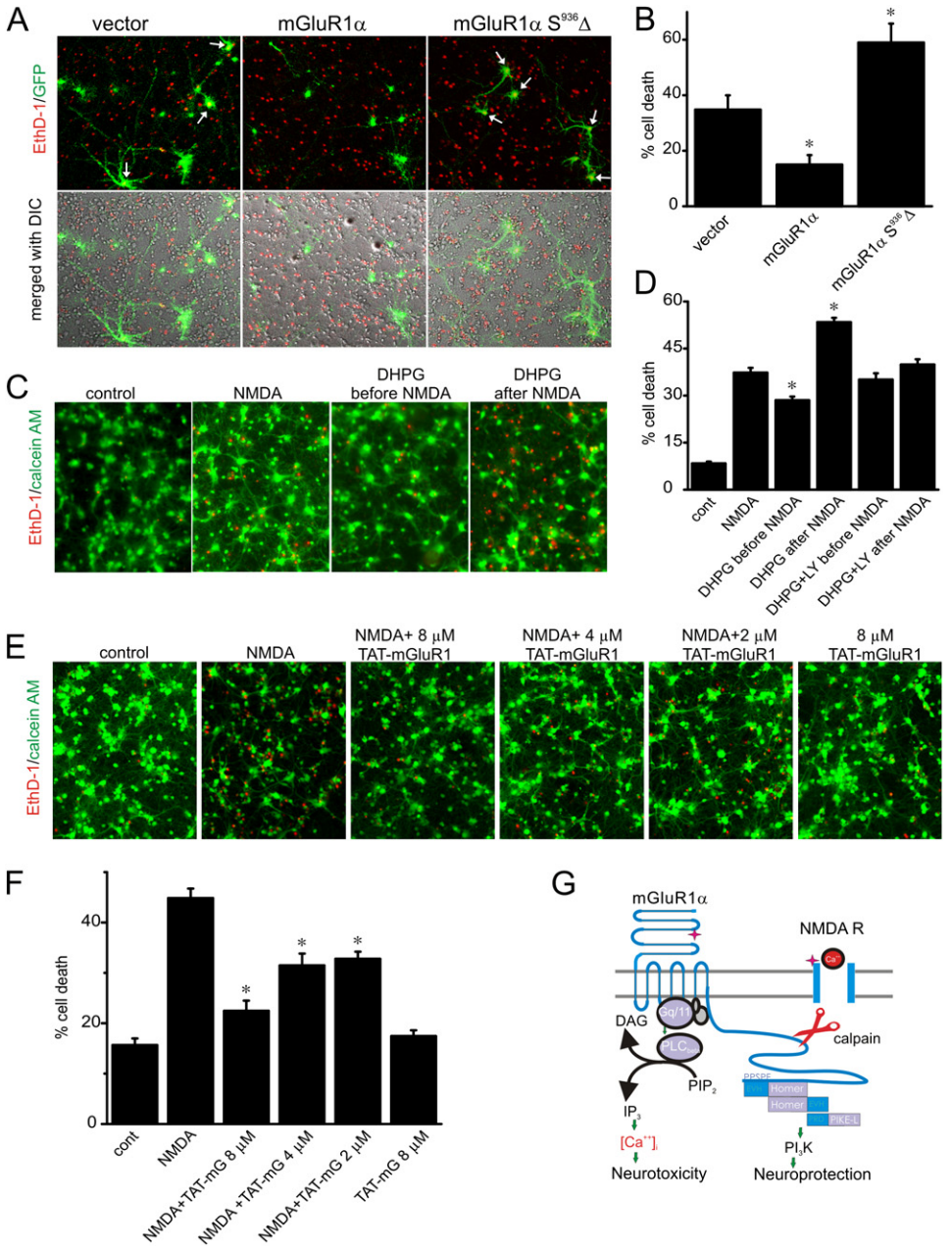


**Figure 6. Distinct Roles of Wild-Type and Truncated mGluR1α in Excitotoxicity**

(A and B) Cortical neurons were cotransfected with GFP and vector DNA, myc-mGluR1α, or myc-mGluR1αS$^{936}$Δ. Two days later, neurons were treated with glutamate and after another 12 hr were stained with EthD-1 to label dead cells. Arrowheads in Figure 7A indicate EthD-1-positive GFP-expressing neurons. *$p < 0.05$.

(C and D) Representative photos and bar graphs showing differential roles for endogenous mGluR1 in neuronal toxicity before and after NMDA-induced truncation. Cortical neurons were treated as indicated (see Results for detailed description) and were stained with EthD-1 and calcein AM (for live cells) 24 hr later. *$p < 0.001$.

(E and F) TAT-mGluR1 peptide protected neurons from NMDA toxicity. Neurons were treated with vehicle or TAT-mGluR1 at the indicated concentrations followed by NMDA. Neurons were stained with EthD-1 and calcein AM 24 hr later. *$p < 0.001$. Results are presented as means ± SEM, Student's t test.

(G) Schematic representation of the alterations in signaling and roles in excitotoxicity of mGluR1α resulting from NMDA receptor-induced calpain-mediated truncation.

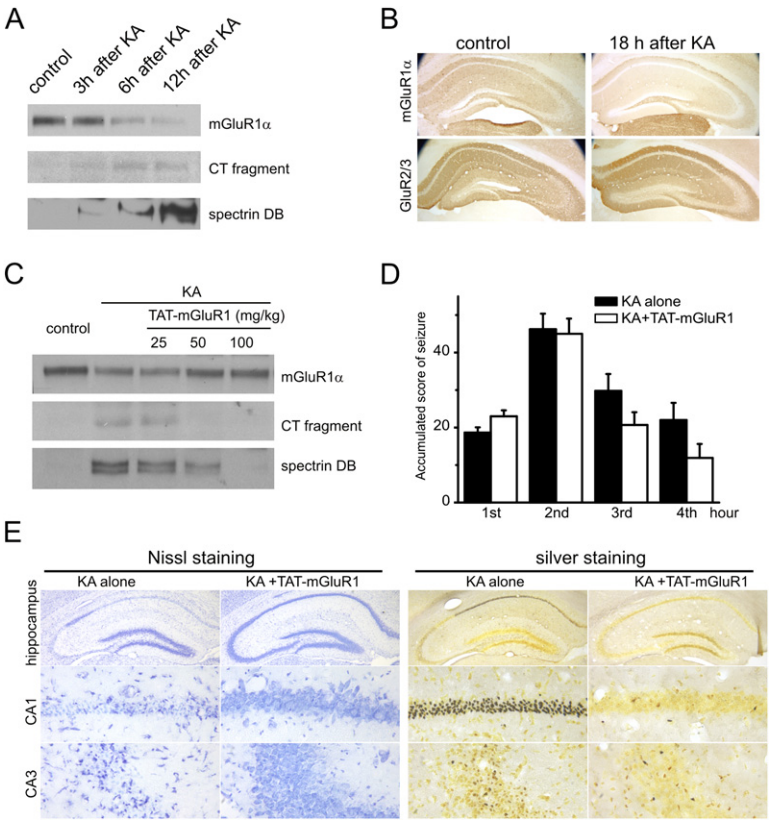


**Figure 7. Truncation of mGluR1α In Vivo**

(A) SD rats were injected with kainic acid. Hippocampi were collected at the indicated times after injection and homogenates were blotted with anti-mGluR1α$_{1142–1160}$ and anti-spectrin.

(B) FVB/N mice were injected with KA and brains were fixed 18 hr after injection. Brain sections were stained with anti-mGluR1α$_{1142–1160}$ and anti-GluR2/3.

(C) TAT-mGluR1 blocked truncation of mGluR1α in vivo. FVB/N mice were injected with vehicle or TAT-mGluR1 at the indicated doses followed by KA injection. Hippocampi were collected 12 hr after KA injection and total homogenates were blotted with anti-mGluR1α$_{1142–1160}$ and anti-spectrin.

(D) TAT-mGluR1 did not affect KA-induced seizures. FVB/N mice were injected (i.p.) with vehicle or TAT-mGluR1 followed by KA. Seizure activity was scored as described in Experimental Procedures. Results are presented as means ± SEM, n = 10–14.

(E) Representative photos showing the neuroprotective effect of TAT-mGluR1 in vivo. Mice were first treated as described in (D). Seven days later, mice were sacrificed and brains were sectioned and processed for Nissl and silver staining.

effects of DHPG before and after NMDA-induced truncation thus demonstrate the distinct roles of full-length and truncated endogenous mGluR1α.

Based on these data, we reasoned that blockade of mGluR1α truncation might have neuroprotective effects. To test this possibility, cortical neurons were incubated with 2, 4, or 8 μM of TAT-mGluR1 peptide or vehicle for 90 min followed by 100 μM of NMDA for 1 hr. Neurons were stained with EthD-1 and calcein AM to determine the percentage of dead cells 24 hr after NMDA treatment. NMDA treatment significantly increased the proportion of dead cells ($p < 0.001$, n = 12–15, Student's t test, NMDA versus cont) (Figures 6D and 6F). Pretreatment with TAT-mGluR1 peptide dose dependently reduced NMDA-induced cell death ($p < 0.001$, n = 9–15, Student's t test for NMDA versus NMDA + TAT-mGluR1 8 μM, NMDA versus NMDA + TAT-mGluR1 4 μM, and NMDA versus NMDA + TAT-mGluR1 2 μM, respectively). The protective effect of TAT-mGluR1 was significant at a concentration as low as 2 μM, where the fusion peptide showed no significant effect on spectrin degradation. These data suggested that neuroprotection can be achieved by blocking mGluR1α truncation.

## Truncation of mGluR1α Contributes to Excitotoxicity In Vivo

To test whether calpain-mediated truncation of mGluR1α occurs with excitotoxicity in vivo, we used kainic acid-induced seizure activity as a model, as neuronal damage resulting from seizures has been shown to be NMDA receptor dependent and calpain activation has also been well documented in this animal model (Siman and Noszek, 1988). Two-month-old male SD rats received systemic injection of kainic acid (KA) (i.p., 12 mg/kg). Hippocampi were collected 3, 6, or 12 hr after injection, homogenized, and processed for immunoblots. As shown in Figure 7A, the 38 kDa C-terminal fragment of mGluR1α was detectable as early as 3 hr after KA injection. At 6 or 12 hr after injection, levels of full-length mGluR1α were significantly reduced. Similarly, the 145 kDa spectrin degradation band was present after KA injection, indicating that calpain was activated. A similar result was obtained in FVB/N mice 12 hr after subcutaneous injection of KA (30 mg/kg) (Figure 7C). Compared with that in cultured neurons, immunoreactivity of the mGluR1α C-terminal fragment after in vivo truncation was relatively weaker. The weaker immunoreactivity of the C-terminal fragment made it possible to determine the location of mGluR1α truncation in vivo with immunohistochemistry. Immunoreactivity for mGluR1α in stratum radiatum of hippocampus, especially in CA1, was significantly reduced following KA injection (Figure 7B). Interestingly, mGluR1α immunostaining in stratum oriens was not reduced or even slightly enhanced, suggesting that mGluR1α truncation might take place mainly in pyramidal cells and not in interneurons located in stratum oriens. GluR2/3 immunoreactivity was not significantly changed except in the CA3 pyramidal cell layer, where immunoreactivity largely disappeared.

To determine whether in vivo truncation of mGluR1α contributes to neuronal degeneration, we used the TAT-mGluR1 fusion peptide to block truncation. FVB/N mice were injected with different concentrations of TAT-mGluR1 fusion peptide (i.p., 25, 50, or 100 mg/kg) or vehicle 90 min before systemic KA injection (s.c., 30 mg/kg). mGluR1α truncation was significantly reduced following treatment with TAT-mGluR1 fusion peptide (50 and 100 mg/kg) (Figure 7C). As was observed in cultured neurons, KA-mediated spectrin degradation was also reduced by peptide treatment. To eliminate the possibility that blockade of calpain activation was due to an effect of the peptide on seizure susceptibility, we analyzed the effects of the fusion peptide on intensity and duration of KA-induced seizure activity. FVB/N mice were injected with 50 mg/kg TAT-mGluR1 peptide or vehicle followed by KA injection 90 min later. We did not observe any behavioral abnormality in mice that received TAT-mGluR1 peptide. Peptide pretreatment did not significantly alter KA-induced seizure ($p > 0.05$, $n = 10–14$, Student's t test for KA alone versus KA + TAT-mGluR1 for each hour, respectively) (Figure 7D). We then tested whether blockade of mGluR1α truncation could protect hippocampal neurons from KA-induced neurodegeneration. Because KA-induced neuron degeneration is closely related to seizure severity, only mice exhibiting stage 5 or higher seizures (see Experimental Procedures for a detailed description of the scale) were used for the cell toxicity experiment. Mice were perfused and fixed 7 days after KA injection. Brains were sectioned and processed for Nissl and silver staining. Representative photos from KA alone or peptide-pretreated (50 mg/kg) mice are shown in Figure 7E. As previously reported in this mouse strain (Schauwecker and Steward, 1997), KA induced severe neurodegeneration in CA1 and CA3, as illustrated by the reduction of Nissl staining and appearance of degenerated neurons in silver staining (degenerated neurons were stained black). Pretreatment with the TAT-mGluR1 peptide significantly reduced KA-induced neurodegeneration, especially in CA1. Among the eight mice injected with KA and vehicle, five exhibited severe neurodegeneration in CA1 and CA3, two mice exhibited moderate neurodegeneration, and only one mouse appeared relatively normal. In contrast, among the eight mice pretreated with TAT-mGluR1 peptide, only two showed moderate neurodegeneration, one showed a low level of neurodegeneration, while the remaining five appeared normal (see Supplemental Data). Together, the data indicate that blockade of mGluR1α truncation in vivo protects neurons from KA-induced degeneration.

## DISCUSSION

### Altered Signaling and Targeting of mGluR1α by Calpain-Mediated Truncation

Calpain is a family of calcium-activated cysteine proteases. μ-calpain and m-calpain are the two calpain isoforms ubiquitously distributed in mammalian cells. Calpain normally induces limited cleavage of substrate proteins to modify rather than abolish their functions (reviewed by Goll et al., 2003). In the central nervous system, calpain is important for neural development, synaptic plasticity, and neural degeneration. Our laboratory previously demonstrated calpain-mediated truncation of both AMPA (Bi et al., 1996) and NMDA receptors (Bi et al., 1998). The present study demonstrates that calpain also truncates the C-terminal domain of mGluR1α.

The mGluR1α signaling mechanism involves the Gq family of heterotrimeric G proteins. The major signal transduction mechanism for mGluR1 consists of activation of phospholipase C (PLC), which hydrolyzes membrane phosphoinositides and leads to $IP_3$-mediated $Ca^{2+}$ release from intracellular stores (Masu et al., 1991). The mGluR1α-G protein coupling involves mainly the second intracellular loop of the receptor (Gomeza et al., 1996); therefore, it is not surprising that mGluR1α remains functional after calpain-mediated truncation, which removes a long fragment from the intracellular C-terminal domain. Besides interacting with G proteins, mGluR1α also directly interacts via its large intracellular C-terminal domain with several other proteins, including Homer family proteins (Fagni et al., 2002), calmodulin and Siah1A (Ishikawa et al., 1999), and membrane channels (Saugstad et al., 1996; Kitano et al., 2003; Kim et al., 2003). The Homer binding motif is located in the distal C terminus of mGluR1α and downstream of the calpain cleavage site. The binding of the receptor to Homer proteins is essential for coupling mGluR1α with the $PI_3$K-Akt system (Rong et al., 2003). Homer proteins also serve as a bridge linking mGluR1α in cell plasma membranes with $IP_3$ receptors in the endoplasmic reticulum membrane and facilitate mGluR-dependent calcium release from intracellular stores (Fagni et al., 2002). As expected, mGluR1-$PI_3$K-Akt signaling was disrupted by calpain-mediated truncation. The mGluR1α-induced calcium transient was also moderately reduced. mGluR1α also gates some membrane channels, such as TRPC1 (Kim et al., 2003) and GIRK1, 2 (Saugstad et al., 1996), which transduce mGluR1α-dependent excitatory postsynaptic current. The detailed mechanism responsible for mGluR1α/membrane channel interactions is largely unknown, and our data indicated that the C-terminal sequence located downstream of the calpain cleavage site is critical for those interactions.

Using immunogold electromicroscopy, Lujan et al. (1996) located mGluR1α to the perisynaptic area of postsynaptic sites. Consistent with this finding, mGluR1α was found to be selectively targeted to dendrites in cultured neurons (Stowell and Craig, 1999). A detailed analysis of mGluR1α targeting revealed two distinct targeting signals in the C-terminal domain, $RRK^{877–879}$ for axonal targeting and another one located in more distal sequences. It has been suggested that the axonal targeting signal is masked by the proximal C terminus (residues 1012–1071) of mGluR1α, resulting in selective delivery of mGluR1α to dendrites (Francesconi and Duvoisin, 2002). In agreement

with this idea, we found that mGluR1αS$^{936}$Δ was preferentially targeted to axons in about 20% of neurons. But unlike the 100% axonal targeting of the short mGluR1 splice variant mGluR1b, mGluR1αS$^{936}$Δ was strictly restricted to cell bodies in the majority of neurons. This finding suggests that, although mGluR1αS$^{936}$Δ is very similar in length to mGluR1b and mGluR1c, it might have different targeting and signaling properties. What governs the differential targeting of mGluR1αS$^{936}$Δ (cell body or axons) in individual neurons is unknown, but such targeting might be due to specific characteristics of neurons (e.g., interneurons versus pyramidal neurons, or neurons derived from different layers or different regions of the cortex).

### Potential Roles of NMDA Receptor/mGluR1 Interactions in Excitotoxicity

NMDA receptors and mGluR1 are colocalized on the postsynaptic membrane and coactivated by glutamate release from presynaptic sites. Functional interactions between these two types of receptors have long been noted (Lan et al., 2001). Physical interactions between the two receptors have also been proposed. It was suggested that mGluR1 could be linked to NMDA receptors through the Homer-Shank-PSD95 complex (Tu et al., 1999) or by Ephrin (Calo et al., 2005). These physical interactions would keep mGluR1 close to NMDA receptor channels and target it for cleavage by locally activated calpain.

Interactions between NMDA and mGluR1 receptors in excitotoxicity appear complicated. Activation of mGluR1 was reported to attenuate NMDA-induced neurotoxicity in cortical neuronal cultures (Koh et al., 1991) and in organotypic hippocampal slice cultures (Baskys et al., 2005). Similarly, pretreatment with mGluRI agonists reduced the excitotoxic effects induced in the retina by intraocular NMDA injection (Siliprandi et al., 1992). However, many studies have indicated that mGluR1 activation exacerbates NMDA receptor-mediated neurotoxicity (Calo et al., 2005; Bruno et al., 1995). Interestingly, activation of mGluR1 before NMDA application tends to be neuroprotective (Blaabjerg et al., 2003), whereas activation of mGluR1 after NMDA application tends to enhance NMDA toxicity (Bruno et al., 1995). Similarly, the protective effects of mGluRI agonists in ischemia are time dependent: they are neuroprotective only when administered before the onset of ischemia (Schroder et al., 1999).

Our findings regarding NMDA-induced mGluR1α truncation provide a possible explanation for these phenomena: before NMDA application or onset of ischemia, mGluR1α receptors are coupled to $PI_3$K-Akt signaling and their activation is neuroprotective. Although mGluR1α activation leads to calcium release from internal stores, the extent of calcium release might be too low and transient to produce significant toxic effects. Following NMDA application or onset of ischemia, NMDA receptor activation induces calpain-mediated truncation of mGluR1α. As a result, the neuroprotective effect of the mGluR1α-$PI_3$K-Akt signaling cascade would be disrupted. In addition, mGluR1α-dependent calcium release from intracellular stores would further contribute to calcium overload due to calcium influx through NMDA receptors and thus enhance neurotoxicity. Finally, because mGluR1 also exhibits presynaptic localization and function (Herrero et al., 1998; Moroni et al., 1998), truncation-mediated mGluR1α translocation to axons might further enhance glutamate release, thereby exacerbating excitotoxicity. Together, NMDA receptor activation followed by calpain-mediated truncation of mGluR1α constitutes a positive feedback loop for excitotoxicity.

Accumulating evidence suggests that calpain also plays a critical role in excitotoxicity. Overactivation of NMDA receptors leads to calpain activation, and calpain blockade protects neurons from excitotoxicity (Higuchi et al., 2005). By cleaving different substrates, calpain triggers multiple neurotoxicity mechanisms. First, by partial truncation of NMDA receptors (Simpkins et al., 2003) and the $Na^+$/Ca exchanger (Bano et al., 2005), calpain enhances calcium overload. Second, through degradation of intracellular antiapoptotic proteins, such as NF-κB (Scholzke et al., 2003), calpain promotes cell-death signaling. Third, by degrading cytoskeleton proteins such as spectrin, calpain disrupts cell structure. In the current study, we show that calpain-mediated mGluR1α truncation plays a critical role in excitotoxicity by both disrupting neuroprotective signaling and enhancing neurotoxic signaling. In the future it will be interesting to test the involvement of this positive feedback loop, namely NMDA receptor/calpain activation/mGluR1α truncation in other models of neurodegeneration where excitotoxicity has been implicated, such as ischemia, Parkinson's disease, and Alzheimer's disease. Moreover, further optimization of the TAT-mGluR1 peptide might provide a very useful tool not only to test this mechanism in these diseases but also to develop new therapeutic treatments.

## EXPERIMENTAL PROCEDURES

### Materials

Monoclonal anti-mGluR1α$_{1142–1160}$ antibody (610965) was obtained from BD Pharmingen (San Diego, CA, USA), anti-myc (ab32) was from Abcam (Cambridge, MA, USA), anti-mGluR5 (06-451) was from Upstate (Charlottesville, VA, USA), anti-VGluT1 (135 302) was from Synaptic Systems (Goettingen, Germany), anti-spectrin (1622) and anti-GluR2/3 (1506) were from Chemicon (Temecula, CA, USA), and anti-phospho-Akt (S473) (AF887) and total Akt (MAB2055) were from R&D Systems (Minneapolis, MN, USA). Human μ-calpain was obtained from Sigma (C6108; St. Louis, MO, USA), calpain inhibitor III (208722) and cpm-VAD-CHO (218830) were from Calbiochem (San Diego, CA, USA), APV, CNQX, DHPG, LY367385, and MPEP were from Tocris (Ellisville, MO, USA), and NVP-AAM077 was a gift from Dr. Yves P. Auberson. TAT peptide was obtained from Anaspec (San Jose, CA, USA). TAT-mGluR1 peptide was synthesized by USC/Norris Comprehensive Cancer Center Core Facilities. The myc-mGluR1α construct was obtained from Dr. Anna Francesconi. GST-mGluR1α fusion proteins were made by subcloning mGluR1α sequences 812–943 or 889–1058 into PEGX 4T-1. mGluR1αS$^{936}$Δ was made by introducing a stop codon right after Ser$^{936}$ of myc-mGluR1α. The constructs were verified by sequencing.

### Cell Cultures and Transfection

Neurons from E18 rat cortex were dissociated and plated in neurobasal medium supplemented with B27, 0.5 mM glutamine, and 12.5 μM glutamate in six-well plates at $10^5$ cells/well for immunostaining and in 60 mm dishes at $1 \times 10^6$ cells/dish for immunoblotting. Neurons were switched to maintenance medium (neurobasal medium supplemented with B27 and 0.5 mM glutamine) the next day and fed twice per week until ready for experiments at 14–18 DIV. Neurons were transfected with a modified calcium phosphate precipitation method (Jiang et al., 2004). HEK293 cells were transfected with Lipofectamine 2000 reagent (Invitrogen, Carlsbad, CA, USA).

### SDS-PAGE and Immunoblotting

Cultured cells or brain tissues were homogenized in boiling lysis buffer (1% SDS, 10 mM Tris, 0.2 mM sodium ortho-vanadate [pH 7.4]). The lysate was denatured at 95°C for 5–10 min, sonicated, and centrifuged at 14,000 rpm for 30 min. Supernatants containing equal amounts of total proteins were processed for SDS-PAGE and immunoblotted with standard chemiluminescence protocols. Blots were digitized and quantified with NIH image software. All band intensities were normalized to that of control samples. For immunoprecipitation, cells were lysed with modified radioimmunoprecipitation buffer and lysates were incubated with anti-myc or anti-mGluR1$\alpha_{1142-1160}$ antibodies. Proteins were pulled down with protein A agarose. Silver staining of SDS gels was conducted with the European Molecular Biology Laboratory silver staining protocol.

### Immunocytochemistry, Immunohistochemistry, and Silver Staining

For immunocytochemistry, neurons were fixed with 4% formaldehyde in PBS (room temperature, 10 min) and permeabilized with 1% Triton X-100 for 5 min. After blocking with 5% goat serum (60 min), neurons were incubated with primary antibodies dissolved in 0.5% goat serum in PBS for 1 hr. Neurons were then incubated with a corresponding fluorescence-tagged secondary antibody for 30 min. For immunohistochemistry, mice were deeply anesthetized with ketamine and xylazine and intracardially perfused with 20 ml chilled PBS (pH 7.4) followed by 100 ml 4% formaldehyde. Brains were removed and postfixed for 2 hr at room temperature. After incubating in PBS with 30% sucrose until sinking, brains were cut into 30 μm thick sections on a cryostat. Free-floating brain sections were immunostained with a VECTASTAIN ABC (standard) kit from Vector Laboratories (Burlingame, CA, USA). Brain-section silver staining was conducted with FD NeuroSilver kit I from FD NeuroTechnologies (Ellicott City, MD, USA) with the manufacturer-provided protocol.

### Electrophysiological Recordings

HEK293 cells plated on poly-D-lysine-coated coverslips were transfected with mGluR1α (either wild-type or truncated form) + TRPC1 + red fluorescent protein (DsRED), or DsRED alone, using lipofectamine (Lipofectamine 2000; Invitrogen). For each well of a 24-well plate, 0.5 μg lipofectamine and cDNAs (0.4 μg mGluR1α + 0.4 μg TRPC1 + 0.1 μg DsRED; DsRED alone, 0.1 μg) were used for transfection. Electrophysiological recording was conducted 48 hr after transfection. In some experiments, TRPC1 was replaced with G protein-coupled inwardly rectifying potassium channel cDNAs (GIRK1 and GIRK2, 0.4 μg each). HEK293 cells on coverslips were transferred to a recording chamber continuously perfused with extracellular solution (ECS) (pH 7.4) containing 140 mM NaCl, 5.4 mM KCl, 1 mM $MgCl_2$, 1.3 mM $CaCl_2$, 25 mM HEPES, and 33 mM glucose. Transfected cells were identified from their DsRED signal under a fluorescence upright microscope. Patch pipettes were pulled from borosilicate glass capillaries (Sutter Instrument Company, Novato, CA, USA) and filled with an intracellular solution (pH 7.2) (300–310 mOsm) composed of 115 mM Cs gluconate, 17.5 mM CsCl, 10 mM HEPES, 2 mM $MgCl_2$, 10 mM EGTA, 4 mM ATP, and 0.1 mM GTP. For GIRK current recordings, the Cs in the intracellular solution was replaced with $K^+$. Recordings of whole-cell currents were obtained following application of DHPG (100 μM) using a fast perfusion system. An Axopatch 200B amplifier (Axon Instruments, Union City, CA, USA) was used for recording. Access resistance was monitored throughout each experiment. Recordings with a series resistance variation of more than 10% were rejected. No electronic compensation for series resistance was used. Whole-cell current recordings were performed in voltage-clamp mode and the membrane potential was maintained at −60 mV. Recorded currents were blocked by the mGluR1 antagonist LY367345 (50 μM; Sigma) (data not shown). Recordings were low-pass filtered at 2 kHz, sampled at 10 kHz, and stored on a PC using Clampex 8.2 (Axon).

### Calcium Imaging

HEK293 cells plated on poly-D-lysine-coated 16 mm coverslips were transfected with mGluR1α (either wild-type or truncated form) + DsRED. Two days after transfection, cells were incubated with a calcium reporter Oregon green 488 BAPTA-1 AM (0.63% in ECS) for 30 min. After washes with ECS, intracellular calcium concentration changes in Oregon green-loaded cells were monitored with a cool CCD camera mounted on a microscope under a 63× objective with the help of Openlab 3.7.5 software (Improvision, Coventry, UK) running on a PowerMac computer. Although all HEK cells were loaded with Oregon green, only 10%–20% of them were mGluR1 transfected so that nontransfected HEK cells in the same visual field could be used as controls. To induce mGluR1-dependent intracellular calcium release, cells were perfused with an extracellular solution containing 100 μM DHPG for 15 s. Images were acquired continuously before and after DHPG application at 5 Hz for 30 s and analyzed offline using Image J software (National Institutes of Health).

### Cell Toxicity Assay

Cell live/dead condition of cultured neurons was assessed with the LIVE/DEAD Viability/Cytotoxicity kit (L-3224; Invitrogen). In this kit, EthD-1 (ethidium homodimer 1, red fluorescent when binding to DNA) is used to stain the nucleus of dead cells with disrupted cell membrane integrity; calcein AM (green fluorescent once it is converted by the esterase of live cells) is used to stain live cells. Cultured cortical neurons were incubated with 0.5 μM EthD-1 and/or 2 μM calcein AM (diluted with neurobasal culture medium) for 10–20 min and washed with neurobasal medium twice before observation under the microscope.

### Behavioral Assessment of KA-Induced Seizure Activity

Seizure activity was assessed with methods described by Holcik et al. (2000) with some modifications. Mice were assigned a score every 5 min after KA injection according to a seven-stage scale: 0 represents normal behavior; 1, immobility; 2, rigid posture; 3, repetitive scratching, circling, or head bobbing; 4, forelimb clonus, rearing, and falling; 5, repeated episodes of level 4 behaviors; 6, severe tonic-clonic behavior; and 7, death. The 12 scores obtained each hour following KA injection were summed to generate the seizure score for that hour. All animal experiments were conducted in accordance with NIH guidelines and protocols approved by the Institutional Animal Care and Use Committee with care to minimize distress to the animals.

### Supplemental Data

Supplemental Data include the effects of mGluR1α point mutations on calpain-mediated truncation and of TAT-mGluR1 peptide on calpain-mediated truncation of mGluR1α in brain membrane fractions and on kainic acid-induced neurodegeneration, and can be found with this article online at http://www.neuron.org/cgi/content/full/53/3/399/DC1/.

## ACKNOWLEDGMENTS

We thank Dr. Hussam Jourdi for comments and suggestions, and Ms. Anna Tran for technical assistance. The pRc-myc-mGluR1α construct was a kind gift from Dr. Anna Francesconi. The TRPC1 construct

was a gift from Dr. Lutz Birnbaumer. We thank Dr. Jean-Philippe Pin for providing us with the mGluR1 and mGluR5 constructs. NVP-AAM077 was a generous gift from Dr. Yves P. Auberson, Novartis. We thank USC/Norris Comprehensive Cancer Center Core Facilities for protein sequencing. This study was supported by NIH grant NS048521-02 from NINDS to M.B.

Received: April 25, 2006
Revised: October 31, 2006
Accepted: December 5, 2006
Published: January 31, 2007

## REFERENCES

Allen, J.W., Eldadah, B.A., and Faden, A.I. (1999). β-amyloid-induced apoptosis of cerebellar granule cells and cortical neurons: exacerbation by selective inhibition of group I metabotropic glutamate receptors. Neuropharmacology *38*, 1243–1252.

Bano, D., Young, K.W., Guerin, C.J., Lefeuvre, R., Rothwell, N.J., Naldini, L., Rizzuto, R., Carafoli, E., and Nicotera, P. (2005). Cleavage of the plasma membrane Na+/$Ca^{2+}$ exchanger in excitotoxicity. Cell *120*, 275–285.

Baskys, A., Bayazitov, I., Fang, L., Blaabjerg, M., Poulsen, F.R., and Zimmer, J. (2005). Group I metabotropic glutamate receptors reduce excitotoxic injury and may facilitate neurogenesis. Neuropharmacology *49* (*Suppl 1*), 146–156.

Bi, X., Chang, V., Molnar, E., McIlhinney, J., and Baudry, M. (1996). The C-terminal domain of GluR1 subunits is a target for calpain-mediated proteolysis. Neuroscience *73*, 903–906.

Bi, X., Chen, J., Dang, S., Wang, Z., and Baudry, M. (1998). Calpain-mediated regulation of NMDA receptor structure and function. Brain Res. *790*, 245–253.

Blaabjerg, M., Fang, L., Zimmer, J., and Baskys, A. (2003). Neuroprotection against NMDA excitotoxicity by group I metabotropic glutamate receptors is associated with reduction of NMDA stimulated currents. Exp. Neurol. *183*, 573–580.

Bruno, V., Copani, A., Knopfel, T., Kuhn, R., Casabona, G., Dell'Albani, P., Condorelli, D.F., and Nicoletti, F. (1995). Activation of metabotropic glutamate receptors coupled to inositol phospholipid hydrolysis amplifies NMDA-induced neuronal degeneration in cultured cortical cells. Neuropharmacology *34*, 1089–1098.

Calo, L., Bruno, V., Spinsanti, P., Molinari, G., Korkhov, V., Esposito, Z., Patane, M., Melchiorri, D., Freissmuth, M., and Nicoletti, F. (2005). Interactions between ephrin-B and metabotropic glutamate 1 receptors in brain tissue and cultured neurons. J. Neurosci. *25*, 2245–2254.

Chong, Z.Z., Li, F., and Maiese, K. (2006). Group I metabotropic receptor neuroprotection requires Akt and its substrates that govern FOXO3a, Bim, and β-catenin during oxidative stress. Curr. Neurovasc. Res. *3*, 107–117.

Fagni, L., Worley, P.F., and Ango, F. (2002). Homer as both a scaffold and transduction molecule. Sci. STKE *2002*, RE8.

Francesconi, A., and Duvoisin, R.M. (2002). Alternative splicing unmasks dendritic and axonal targeting signals in metabotropic glutamate receptor 1. J. Neurosci. *22*, 2196–2205.

Goll, D.E., Thompson, V.F., Li, H., Wei, W., and Cong, J. (2003). The calpain system. Physiol. Rev. *83*, 731–801.

Gomeza, J., Joly, C., Kuhn, R., Knopfel, T., Bockaert, J., and Pin, J.P. (1996). The second intracellular loop of metabotropic glutamate receptor 1 cooperates with the other intracellular domains to control coupling to G-proteins. J. Biol. Chem. *271*, 2199–2205.

Herrero, I., Miras-Portugal, M.T., and Sanchez-Prieto, J. (1998). Functional switch from facilitation to inhibition in the control of glutamate release by metabotropic glutamate receptors. J. Biol. Chem. *273*, 1951–1958.

Higuchi, M., Tomioka, M., Takano, J., Shirotani, K., Iwata, N., Masumoto, H., Maki, M., Itohara, S., and Saido, T.C. (2005). Distinct mechanistic roles of calpain and caspase activation in neurodegeneration as revealed in mice overexpressing their specific inhibitors. J. Biol. Chem. *280*, 15229–15237.

Holcik, M., Thompson, C.S., Yaraghi, Z., Lefebvre, C.A., MacKenzie, A.E., and Korneluk, R.G. (2000). The hippocampal neurons of neuronal apoptosis inhibitory protein 1 (NAIP1)-deleted mice display increased vulnerability to kainic acid-induced injury. Proc. Natl. Acad. Sci. USA *97*, 2286–2290.

Hou, L., and Klann, E. (2004). Activation of the phosphoinositide 3-kinase-Akt-mammalian target of rapamycin signaling pathway is required for metabotropic glutamate receptor-dependent long-term depression. J. Neurosci. *24*, 6352–6361.

Ishikawa, K., Nash, S.R., Nishimune, A., Neki, A., Kaneko, S., and Nakanishi, S. (1999). Competitive interaction of seven in absentia homolog-1A and $Ca^{2+}$/calmodulin with the cytoplasmic tail of group 1 metabotropic glutamate receptors. Genes Cells *4*, 381–390.

Jiang, M., Deng, L., and Chen, G. (2004). High Ca($^{2+}$)-phosphate transfection efficiency enables single neuron gene analysis. Gene Ther. *11*, 1303–1311.

Kim, S.J., Kim, Y.S., Yuan, J.P., Petralia, R.S., Worley, P.F., and Linden, D.J. (2003). Activation of the TRPC1 cation channel by metabotropic glutamate receptor mGluR1. Nature *426*, 285–291.

Kitano, J., Nishida, M., Itsukaichi, Y., Minami, I., Ogawa, M., Hirano, T., Mori, Y., and Nakanishi, S. (2003). Direct interaction and functional coupling between metabotropic glutamate receptor subtype 1 and voltage-sensitive Cav2.1 $Ca^{2+}$ channel. J. Biol. Chem. *278*, 25101–25108.

Koh, J.Y., Palmer, E., and Cotman, C.W. (1991). Activation of the metabotropic glutamate receptor attenuates N-methyl-D-aspartate neurotoxicity in cortical cultures. Proc. Natl. Acad. Sci. USA *88*, 9431–9435.

Lan, J.Y., Skeberdis, V.A., Jover, T., Zheng, X., Bennett, M.V., and Zukin, R.S. (2001). Activation of metabotropic glutamate receptor 1 accelerates NMDA receptor trafficking. J. Neurosci. *21*, 6058–6068.

Lujan, R., Nusser, Z., Roberts, J.D., Shigemoto, R., and Somogyi, P. (1996). Perisynaptic location of metabotropic glutamate receptors mGluR1 and mGluR5 on dendrites and dendritic spines in the rat hippocampus. Eur. J. Neurosci. *8*, 1488–1500.

Masu, M., Tanabe, Y., Tsuchida, K., Shigemoto, R., and Nakanishi, S. (1991). Sequence and expression of a metabotropic glutamate receptor. Nature *349*, 760–765.

Moroni, F., Cozzi, A., Lombardi, G., Sourtcheva, S., Leonardi, P., Carfi, M., and Pellicciari, R. (1998). Presynaptic mGlu1 type receptors potentiate transmitter output in the rat cortex. Eur. J. Pharmacol. *347*, 189–195.

Newcomb, J.K., Pike, B.R., Zhao, X., and Hayes, R.L. (2000). Concurrent assessment of calpain and caspase-3 activity by means of western blots of protease-specific spectrin breakdown products. Methods Mol. Biol. *144*, 219–223.

Pellegrini-Giampietro, D.E. (2003). The distinct role of mGlu1 receptors in post-ischemic neuronal death. Trends Pharmacol. Sci. *24*, 461–470.

Rong, R., Ahn, J.Y., Huang, H., Nagata, E., Kalman, D., Kapp, J.A., Tu, J., Worley, P.F., Snyder, S.H., and Ye, K. (2003). $PI_3$ kinase enhancer-Homer complex couples mGluRI to $PI_3$ kinase, preventing neuronal apoptosis. Nat. Neurosci. *6*, 1153–1161.

Sagara, Y., and Schubert, D. (1998). The activation of metabotropic glutamate receptors protects nerve cells from oxidative stress. J. Neurosci. *18*, 6662–6671.

Saugstad, J.A., Segerson, T.P., and Westbrook, G.L. (1996). Metabotropic glutamate receptors activate G-protein-coupled inwardly rectifying potassium channels in *Xenopus* oocytes. J. Neurosci. *16*, 5979–5985.

Schauwecker, P.E., and Steward, O. (1997). Genetic determinants of susceptibility to excitotoxic cell death: implications for gene targeting approaches. Proc. Natl. Acad. Sci. USA *94*, 4103–4108.

Scholzke, M.N., Potrovita, I., Subramaniam, S., Prinz, S., and Schwaninger, M. (2003). Glutamate activates NF-κB through calpain in neurons. Eur. J. Neurosci. *18*, 3305–3310.

Schroder, U.H., Opitz, T., Jager, T., Sabelhaus, C.F., Breder, J., and Reymann, K.G. (1999). Protective effect of group I metabotropic glutamate receptor activation against hypoxic/hypoglycemic injury in rat hippocampal slices: timing and involvement of protein kinase C. Neuropharmacology *38*, 209–216.

Siliprandi, R., Lipartiti, M., Fadda, E., Sautter, J., and Manev, H. (1992). Activation of the glutamate metabotropic receptor protects retina against N-methyl-D-aspartate toxicity. Eur. J. Pharmacol. *219*, 173–174.

Siman, R., and Noszek, J.C. (1988). Excitatory amino acids activate calpain I and induce structural protein breakdown in vivo. Neuron *1*, 279–287.

Simpkins, K.L., Guttmann, R.P., Dong, Y., Chen, Z., Sokol, S., Neumar, R.W., and Lynch, D.R. (2003). Selective activation induced cleavage of the NR2B subunit by calpain. J. Neurosci. *23*, 11322–11331.

Stowell, J.N., and Craig, A.M. (1999). Axon/dendrite targeting of metabotropic glutamate receptors by their cytoplasmic carboxy-terminal domains. Neuron *22*, 525–536.

Tu, J.C., Xiao, B., Naisbitt, S., Yuan, J.P., Petralia, R.S., Brakeman, P., Doan, A., Aakalu, V.K., Lanahan, A.A., Sheng, M., and Worley, P.F. (1999). Coupling of mGluR/Homer and PSD-95 complexes by the Shank family of postsynaptic density proteins. Neuron *23*, 583–592.

Vincent, A.M., and Maiese, K. (2000). The metabotropic glutamate system promotes neuronal survival through distinct pathways of programmed cell death. Exp. Neurol. *166*, 65–82.

Wadia, J.S., Stan, R.V., and Dowdy, S.F. (2004). Transducible TAT-HA fusogenic peptide enhances escape of TAT-fusion proteins after lipid raft macropinocytosis. Nat. Med. *10*, 310–315.

Zhu, P., DeCoster, M.A., and Bazan, N.G. (2004). Interplay among platelet-activating factor, oxidative stress, and group I metabotropic glutamate receptors modulates neuronal survival. J. Neurosci. Res. *77*, 525–531.